

3-D prestack depth migration of common-azimuth data

*Biondo Biondi and Gopal Palacharla*¹

ABSTRACT

We extended the common-azimuth 3-D prestack migration method presented in a previous report (Biondi and Palacharla, 1994a) to the important case of imaging common-azimuth data when the velocity field varies laterally. This generalization leads to an efficient mixed space-wavenumber domain algorithm for 3-D prestack depth migration of common-azimuth data. We implemented the method using a split-step scheme, and applied it to the migration of two synthetic data sets: the first data set was generated assuming a vertical velocity gradient, the second one assuming a velocity gradient with both a vertical and a horizontal component. Common-azimuth migration correctly imaged the reflectors in both cases.

INTRODUCTION

For 3-D prestack migration, Kirchhoff methods are usually preferred over methods based on recursive downward continuation because of their flexibility in handling 3-D prestack data geometries (Audebert, 1994). Kirchhoff methods can be employed to efficiently migrate data sets with uneven spatial sampling and data sets that are subsets of the complete prestack data, such as common-offset cubes and common-azimuth cubes. For recursive methods the irregular sampling problem can be addressed with an interpolation preprocessing step, though in practice it can be a challenging task. However, in principle the downward continuation of prestack subsets should be carried out in the full 5-D data space, even when the original subset is 3-D (common offset) or 4-D (common azimuth). As a result of these constraints on the dimensionality of the computational domain, most of the computations are wasted on propagating components of the wavefield that either are equal to zero or do not contribute to the final image. These potential limitations of recursive methods have led the industry to adopt almost exclusively Kirchhoff methods for 3-D prestack migration (Western and Ball, 1991; Ratcliff et al., 1994), though recursive methods have some intrinsic advantages over Kirchhoff methods. First, they are potentially more accurate and robust because they are based on the full wave-equation and not on an asymptotic solution based on ray theory. Second, when they can be used to extrapolate the recorded data without increasing their dimensionality (e.g. zero-offset data), they can be implemented more efficiently than the corresponding Kirchhoff methods.

In a previous report (Biondi and Palacharla, 1994a) we introduced a method for efficiently

¹email: biondo@sep.stanford.edu,gopal@sep.stanford.edu

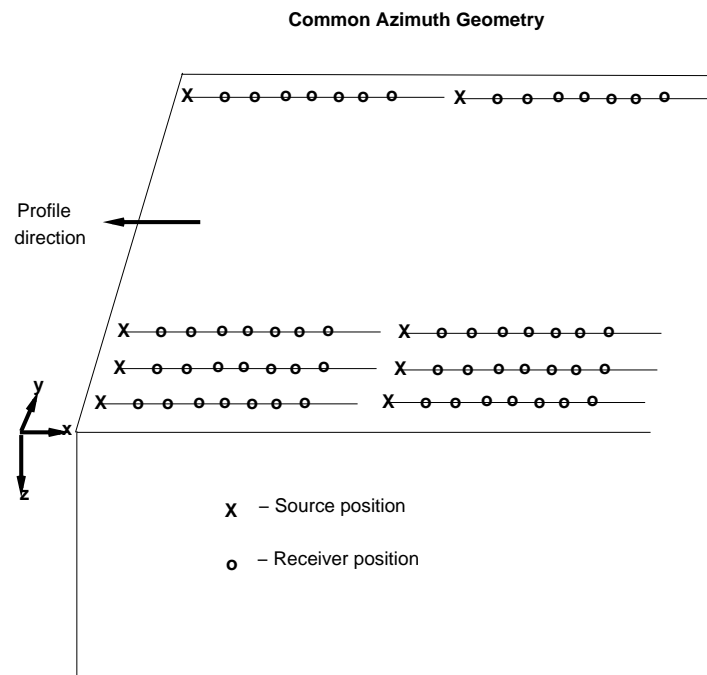


Figure 1: Schematic showing the acquisition geometry of common-azimuth data. The data are acquired along parallel lines, with all the offset vectors aligned along a common azimuth. For simplicity, but without loss of generality, we assume that the common offset-azimuth is aligned along the in-line direction. biondo1-acquis [NR]

migrating common-azimuth data (see Figure ?? for a schematic representation of common-azimuth acquisition geometry) by recursive downward continuation in the original 4-D space. An efficient algorithm for migrating common-azimuth subsets has useful practical applications because common-azimuth data are either the result of a collection of actual physical experiments (e.g. single-streamer marine survey with negligible cable feather) or they may be synthesized by preprocessing (Biondi and Chemingui, 1994). However, in the previous report we applied common-azimuth migration to the case of limited interest when velocity varies only with depth; we did not address the important issue of applying the method to the general case when the velocity function is laterally varying. Similarly, Ikelle (1991) developed (unknown to us at the time we wrote the first report) a linearized inversion method for common-azimuth data that shares with our previous work the same theoretical basis, but also shares the same limitations of applicability to a medium with only vertical velocity variations. In this paper, we overcome these limitations and we generalize common-azimuth migration to the case of laterally varying velocity.

The generalization of common-azimuth migration presented in this paper is based on two new theoretical insights. First, we derive common-azimuth migration as a recursive downward continuation by a new operator that continues common-azimuth data recorded at one depth level to common-azimuth data recorded at the next depth level. The previous derivation of common-azimuth migration was based on stationary-phase approximation to the whole process of downward continuation followed by imaging at zero offset. Isolating the common-azimuth downward continuation from imaging enables us to better understand the assumptions underlying common-azimuth migration. The second improvement in the theory follows from a ray-based geometric interpretation of common-azimuth downward continuation. Thanks to this ray interpretation we derived and justified a more general formulation of the stationary-phase result that can be applied to downward continuation in presence of lateral velocity variations. Furthermore, the geometric insight enables us to analyze the errors caused by the use of common-azimuth continuation in place of full 3-D prestack continuation and to gain an appreciation of the limitations and strengths of the proposed method.

COMMON-AZIMUTH DOWNWARD CONTINUATION

We first derive a wave-equation operator for downward continuing common-azimuth data by applying a stationary phase approximation to the frequency-wavenumber domain formulation of the full 3-D prestack downward continuation operator. Then, we present a ray-based geometric interpretation of the stationary-phase result, and use this geometric interpretation to generalize the frequency-wavenumber results to a medium where the velocity function varies laterally, and to analyze the errors caused by the use of common-azimuth continuation in the presence of lateral velocity variations.

The acquisition geometry of common-azimuth data is shown in Figure ?. Without loss of generality we assume that the common offset-azimuth is aligned with the x axis (in-line axis). Since the offset vectors between source and receivers are constrained to have the same azimuth, common-azimuth data has only four dimensions. The four axes are: recording time,

two midpoints, and the offset along the azimuthal direction. A common azimuth data set can be downward continued by applying the full 3-D prestack downward continuation operator, that in the frequency-wavenumber domain can be expressed as a phase-shift operator, with the phase given by the 3-D double square root equation (DSR). In 3-D the DSR equation is a function of five scalar variables: the temporal frequency (ω), the two components of the midpoint wavenumber vector ($\mathbf{k}_m = k_{mx}\mathbf{x}_m + k_{my}\mathbf{y}_m$), and the two components of the offset wavenumber evaluation of the phase function ($\mathbf{k}_h = k_{hx}\mathbf{x}_h + k_{hy}\mathbf{y}_h$). The downward continuation of common-azimuth $CA(\omega, \mathbf{k}_m, k_{hx})$ data from depth z to depth $z + dz$ by full 3-D prestack continuation can be expressed as

$$D_{z+dz}(\omega, \mathbf{k}_m, \mathbf{k}_h) = CA_z(\omega, \mathbf{k}_m, k_{hx})e^{-i\Phi(\omega, \mathbf{k}_m, \mathbf{k}_h, z)}, \quad (1)$$

where the phase function is given by

$$\Phi(\omega, \mathbf{k}_m, \mathbf{k}_h, z) = DSR(\omega, \mathbf{k}_m, \mathbf{k}_h, z)dz, \quad (2)$$

and the double-square root equation is equal to

$$\begin{aligned} & DSR(\omega, \mathbf{k}_m, \mathbf{k}_h, z) \\ &= \omega \left\{ \sqrt{\frac{1}{v(\mathbf{r}, z)^2} - \frac{1}{4\omega^2}[(k_{mx} + k_{hx})^2 + (k_{my} + k_{hy})^2]} + \right. \\ & \quad \left. \sqrt{\frac{1}{v(\mathbf{s}, z)^2} - \frac{1}{4\omega^2}[(k_{mx} - k_{hx})^2 + (k_{my} - k_{hy})^2]} \right\}, \quad (3) \end{aligned}$$

where $v(\mathbf{s}, z)$ and $v(\mathbf{r}, z)$ are the velocities evaluated respectively at the source and receiver locations at depth z . The distinction between velocity at the source and velocity at the receiver may seem somewhat artificial in the wavenumber domain, but it is important to keep them as two separate parameters during the stationary-phase approximation to derive a method applicable to depth migration. A physical interpretation of the significance of the source and receiver velocity terms is possible after the geometric interpretation of the stationary-phase results presented in the next section.

The result of the downward continuation with the full 3-D prestack is five dimensional, although the original common-azimuth data is only four dimensional. This increase in the dimensionality of the computational domain causes a drastic increase in the computational and memory requirements of 3-D prestack downward continuation, making it unattractive compared with other migration methods, such as the ones based on the Kirchhoff integral. However, the computational cost can be greatly reduced by applying a new downward continuation operator that evaluates the wavefield at the new depth level only along the offset-azimuth of the original data. We derive this operator by evaluating the data at the new depth level ($z + dz$) at the origin of the cross-line offset axis ($hy = 0$) by integration over the cross-line offset wavenumber,

$$\begin{aligned} & CA_{z+dz}(\omega, \mathbf{k}_m, k_{hx}) \\ &= \int_{-\infty}^{+\infty} dk_{hy} CA_z(\omega, \mathbf{k}_m, k_{hx})e^{-i\Phi(\omega, \mathbf{k}_m, \mathbf{k}_h, z)} \\ &= CA_z(\omega, \mathbf{k}_m, k_{hx}) \left\{ \int_{-\infty}^{+\infty} dk_{hy} e^{-i\Phi(\omega, \mathbf{k}_m, \mathbf{k}_h, z)} \right\}, \quad (4) \end{aligned}$$

and by recognizing that since common-azimuth data is independent of k_{hy} the integral can be pulled inside and analytically approximated by the stationary phase method (Bleistein, 1984). The common-azimuth downward continuation operator can thus be written as

$$Down(\omega, \mathbf{k}_m, k_{hx}, z) = \frac{2\pi}{\sqrt{\Phi''_{stat}(\omega, \mathbf{k}_m, k_{hx}, z)}} e^{-i\Phi_{stat}(\omega, \mathbf{k}_m, k_{hx}, z) + i\frac{\pi}{4}}. \quad (5)$$

The phase function Φ_{stat} is equal to the phase function in equation (2) evaluated along the stationary path, and is equal to

$$\Phi_{stat}(\omega, \mathbf{k}_m, k_{hx}, z) = DSR \left[\omega, \mathbf{k}_m, k_{hx}, k'_{hy}(z), z \right] dz; \quad (6)$$

where and $k'_{hy}(z)$ is the stationary path for the double-square root equation, as a function of k_{hy} . There are two solutions for the stationary path of the double-square root equation; they are

$$\hat{k}'_{hy}(z) = k_{my} \frac{\sqrt{\frac{1}{v(\mathbf{r}, z)^2} - \frac{1}{4\omega^2} (k_{mx} + k_{hx})^2} \mp \sqrt{\frac{1}{v(\mathbf{s}, z)^2} - \frac{1}{4\omega^2} (k_{mx} - k_{hx})^2}}{\sqrt{\frac{1}{v(\mathbf{r}, z)^2} - \frac{1}{4\omega^2} (k_{mx} + k_{hx})^2} \pm \sqrt{\frac{1}{v(\mathbf{s}, z)^2} - \frac{1}{4\omega^2} (k_{mx} - k_{hx})^2}}. \quad (7)$$

In choosing between these two solutions, we first notice that one solution is the inverse of the other. Second we consider the limiting case of the in-line offset wavenumber (k_{hx}) equal to zero. In this case one solution diverges while the other (being the one with the minus sign at the numerator) is equal to zero. We accept this second solution because it is consistent with the notion that when both k_{hx} and k_{hy} vanish the double square root equation reduces to the single square root equation that is commonly used for migrating zero-offset data (Claerbout, 1985).

The implementation of common-azimuth downward continuation as described by equation (3) through equation (7) yields an algorithm for efficient migration of common-azimuth data. When the velocity field is only a function of depth the method can be efficiently implemented by a simple phase-shift algorithm. When the velocity field is also function of the lateral coordinates, and accurate depth-migration is required, the method should be implemented using a mixed space-wavenumber domain migration scheme, such as Phase-Shift Plus Interpolation (PSPI) (Gazdag and Sguazzero, 1984) or split step (Stoffa et al., 1990). We implemented the equations using a straightforward generalization of split step to prestack migration because of its simplicity and computational efficiency; other choices would have probably been just as effective.

In the next two sections, we analyze common-azimuth downward continuation by using a ray-theoretical interpretation of the method. The goal is to understand the underlying assumptions, and to understand the accuracy limitation of the method when velocity variations cause ray bending.

Geometric interpretation of common-azimuth downward continuation

The common-azimuth downward continuation operator derived by stationary phase has a straightforward geometric interpretation in terms of propagation directions of the rays of the

continued wavefield. In Appendix A we show that expression for the stationary path of equation (7) is equivalent to the relationship

$$\frac{p_{sy}}{p_{sz}} = \frac{p_{ry}}{p_{rz}}, \quad (8)$$

among the ray parameters for the rays downward propagating the sources (p_{sx}, p_{sy}, p_{sz}) and the ray parameters for the rays downward propagating the receivers (p_{rx}, p_{ry}, p_{rz}) . This relationship between the ray parameters constrains the direction of propagation of the source and receiver rays, for each possible pair of rays. In particular, the source ray and the receiver ray must lie on the same plane; with all the possible propagation planes sharing the line that connects the source and receiver location at each depth level. This geometric relationship constrains the sources and receivers at the new depth level to be aligned along the same azimuth as the source and receivers at the previous depth level, consistently with the condition that we imposed for the stationary phase derivation of the common-azimuth downward continuation operator [equation (4)]. Figure ?? shows a graphical representation of the geometric interpretation of common-azimuth downward continuation. The source ray and the receiver ray must lie on any of the slanted planes that share the line connecting the source and receiver locations.

In Appendix A we show that from equation (8) it is possible to derive the ray parameter equivalent of the stationary-path expression of equation (7); that is,

$$(p_{ry} - p_{sy}) = (p_{ry} + p_{sy}) \frac{\sqrt{\frac{1}{v(\mathbf{r},z)^2} - p_{rx}^2} - \sqrt{\frac{1}{v(\mathbf{s},z)^2} - p_{sx}^2}}{\sqrt{\frac{1}{v(\mathbf{r},z)^2} - p_{rx}^2} + \sqrt{\frac{1}{v(\mathbf{s},z)^2} - p_{sx}^2}}. \quad (9)$$

In this expression the distinction between the velocity at the source location, and the velocity at the receiver location introduced in equation (3), and formally carried through the stationary phase approximation, is now physically meaningful. It implies that the source rays and receiver rays must lie on the same plane, notwithstanding different local velocities and ray bending.

Common-azimuth downward continuation and ray bending

As we previously discussed (Biondi and Palacharla, 1994b), when the propagation velocity is constant common-azimuth downward continuation is exact, within the limits of the stationary-phase approximation. In this case, there is no ray bending and the source and receiver rays propagate straight along the slanted planes shown in Figure ?? at every depth level, until they meet to image a diffractor at depth. However, when ray bending occurs, it seems that common-azimuth downward continuation introduces an error. This conclusion would be in contradiction with the accurate results obtained by the application of common-azimuth migration shown in the next section, and it requires a closer examination. We first discuss the simpler case of velocity varying with depth, and then the general case of velocity varying laterally.

Inspection of the stationary-phase results [equation (7) and equation (9)] shows that in a horizontally stratified medium the cross-line ray parameters for the source and receiver rays

(p_{sy}, p_{ry}) change across boundaries between layers with different velocities. This result contradicts Snell's law that states that the horizontal ray parameters must be constant when the velocity varies only vertically. In common-azimuth downward continuation, by imposing the constraint that the source and receiver ray must lie on the same plane, we force the source and receiver rays to bend across interfaces in a way that may not be consistent with Snell's law. In particular, the ray bending determined by common-azimuth continuation is incorrect when the velocity variations would prescribe the source ray to bend differently than the receiver ray along the cross-line direction. This error in the ray bending can be analyzed by evaluating the difference between the values of $(p_{ry} - p_{sy})$ across an interface where the upper layer has velocity V_1 and the lower layer has velocity V_2

$$\begin{aligned} \Delta(p_{ry} - p_{sy}) &= \Delta\left(\frac{\hat{k}'_{hy}(z)}{\omega}\right) \\ &= 2(p_{ry} + p_{sy}) \frac{\sqrt{\frac{1}{V_1^2} - p_{sx}^2} \sqrt{\frac{1}{V_2^2} - p_{rx}^2} - \sqrt{\frac{1}{V_1^2} - p_{rx}^2} \sqrt{\frac{1}{V_2^2} - p_{sx}^2}}{\left(\sqrt{\frac{1}{V_1^2} - p_{rx}^2} + \sqrt{\frac{1}{V_1^2} - p_{sx}^2}\right) \left(\sqrt{\frac{1}{V_2^2} - p_{rx}^2} + \sqrt{\frac{1}{V_2^2} - p_{sx}^2}\right)}. \end{aligned} \quad (10)$$

It is straightforward to show from (10) that the error is equal to zero, if and only if, one of the following conditions is fulfilled,

$$|p_{rx}| = |p_{sx}| \quad (11)$$

$$p_{ry} = -p_{sy} \quad (12)$$

$$V_1 = V_2 \quad . \quad (13)$$

The first condition is fulfilled when either the source ray is parallel to the receiver ray (e.g. zero offset data), or the two rays converge and form opposite angles with the in-line axis x (e.g. flat reflections along the in-line midpoint axis). The second condition is fulfilled in the case of vertical propagation (2-D), while the third condition confirms that when the velocity is constant common-azimuth downward continuation is kinematically exact.

The previous analysis shows that common-azimuth downward continuation introduces an error in the ray bending across velocity interfaces. However, this consideration does not necessarily lead to the conclusion that common-azimuth continuation is inaccurate. On the contrary, we argue that the error in the ray bending causes only second order errors in the continuation results. This claim can be simply verified by recognizing that for downward continuing common-azimuth data we evaluate the phase function $\Phi(\omega, \mathbf{k}_m, \mathbf{k}_h, z)$ [equation (3)] at its stationary point $\hat{k}'_{hy}(z)$ [equation (7)] with respect to the cross-line offset wavenumber k_{hy} . Since the phase function is stationary at $\hat{k}'_{hy}(z)$ the first order term of its Taylor expansion as a function of k_{hy} around $\hat{k}'_{hy}(z)$ is equal to zero. Therefore, an error in k_{hy} has only a second order effect on the evaluation of the phase function $\Phi_{stat}(\omega, \mathbf{k}_m, k_{hx}, z)$ [equation (6)]. In other words, the error introduced by the incorrect ray bending has second order effects on the continuation results, and consequently on the migration results. This conclusion is supported by the accuracy of the migrated images shown in the next section.

When the velocity field varies laterally, the previous analysis becomes more complex because the incorrect ray bending causes errors in the evaluation of the phase function not only

through errors in the cross-line offset wavenumber $\hat{k}'_{hy}(z)$, but also through errors in the horizontal locations where the velocity function is evaluated. The arguments that support the conclusion that the errors in the phase function caused by error in $\hat{k}'_{hy}(z)$ are of second order are still valid for the general case of lateral velocity variations. However, the magnitude of the error introduced by the mispositioning of sources and receivers at depth when evaluating the velocity function cannot be neglected in principle. These errors are dependent on the spatial variability of the velocity function, and cannot be readily analyzed analytically. In the following section we show accurate migration results obtained over a velocity function varying both laterally and vertically. These results are encouraging and suggest that the range of application of common-azimuth migration to depth migration problems is fairly large.

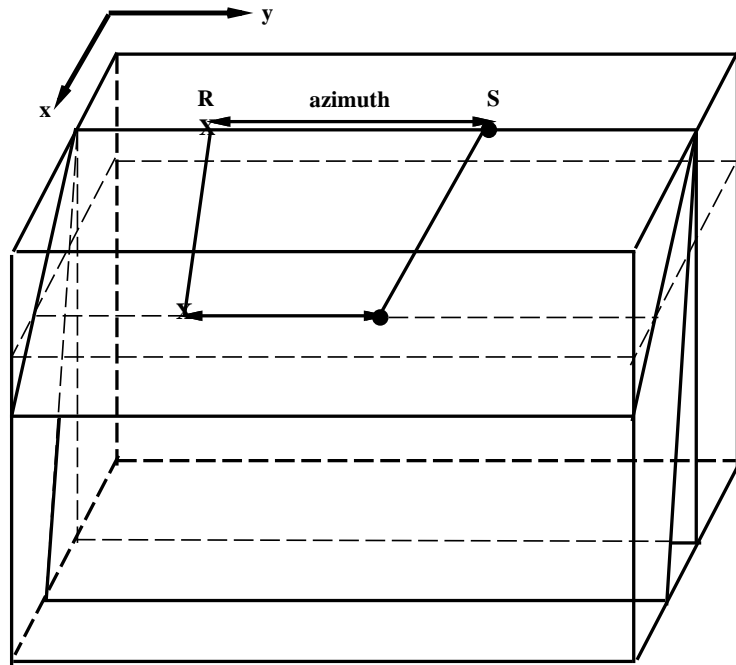


Figure 2: Schematic showing the ray geometry for common-azimuth downward continuation. For each pair of source ray and receiver ray, both rays are constrained to lie on the same slanted plane. All the propagation planes share the line connecting the source and the receiver locations. `biondo1-stconv` [NR]

MIGRATION RESULTS

We tested common-azimuth migration by imaging two synthetic data sets generated by a modeling program based on the Kirchhoff integral. The Green functions are computed analytically assuming velocity functions with a constant spatial gradient. In both cases the velocity at the origin of the spatial coordinates is equal to 1.7 km s^{-1} . The first data set is generated assuming a vertical gradient of 1.0 s^{-1} while the second data set is generated assuming a gradient with the horizontal component equal to 0.2 s^{-1} and the vertical component equal to 0.25 s^{-1} .

The horizontal component of the gradient is oriented at an angle of 45 degrees with respect to the offset azimuth (in-line direction) of the acquisition geometry. The reflectivity model is a constant reflectivity function positioned along a half-spherical dome superimposed onto a horizontal planar reflector.

The acquisition geometry has 128 midpoint along both the in-line and cross-line directions; with midpoint spacing of 25 m in both directions. Each midpoint gather has 64 offsets, spaced every 40 m; the nearest offset traces are actually recorded at zero offset. The offset-azimuth of the data is aligned with the in-line direction. Figure ?? and ?? show two in-line zero-offset sections extracted from respectively the vertical gradient data set and the oblique gradient data set. The effects of the lateral component of the velocity gradient are evident in both the tilting of the horizontal reflector, and in the asymmetry of the quasi-hyperbolic reflections from the dome.

Figures ?? and ?? show an in-line section and a depth slice of the results of migrating the vertical gradient data set. The in-line section (Figure ??) is taken across the middle of the dome, while the depth slice (Figure ??) is taken across the base of the dome ($z = 1.75$ km). Common-azimuth migration has accurately imaged the data; both the in-line section and the depth slice show a perfect focusing of the reflectors. To visually verify the isotropic response of common-azimuth migration we overlaid a circle onto the depth slice. The migrated dome is perfectly circular, notwithstanding the ray bending caused by the strong vertical velocity gradient.

Figures ?? and ?? show the result of migrating the oblique gradient data set. The in-line section (Figure ??) shows that common-azimuth migration has correctly positioned the reflectors. The planar reflector has been flattened, and the spherical dome has been properly focused. A spatial variability in both the frequency content and the amplitude of the migrated reflector is noticeable in the depth slice. The frequency variability is expected, and it is caused by the widening of the spatial wavelength of the wavefield caused by higher propagation velocities. The wavelet is narrower closer to the origin (upper-left corner) where velocity is lower and it is wider where the velocity is higher (lower-right corner). The amplitude variations cannot be readily explained, and further analysis is needed to determine whether they are artifacts of common-azimuth migration. The combined frequency and amplitude effects creates an “anisotropic” appearance to the migrated image. However, by overlaying a circle onto the plot of the seismic data we see that the migrated dome, though not perfectly circular, it is very close to circular. The comparison of these results with the results from the vertical gradient data set confirm the accuracy of common-azimuth migration even in the presence of strong lateral velocity gradients.

CONCLUSIONS

We have shown that common-azimuth migration (Biondi and Palacharla, 1994b) can be successfully applied to imaging 3-D prestack data with laterally varying velocity. This important generalization of common-azimuth migration was made possible by two theoretical insights. The first one led us to recast common-azimuth migration as a recursive application of a new



Figure 3: In-line zero-offset section extracted from the synthetic data set modeled assuming a constant vertical gradient in velocity equal to 1.0 s^{-1} .



Figure 4: In-line zero-offset section extracted from the synthetic data set modeled assuming a constant velocity gradient with the horizontal component equal to 0.2 s^{-1} and the vertical component equal to 0.25 s^{-1} .



Figure 5: In-line section of the migration results for the vertical gradient data set. This section passes through the middle of the dome.

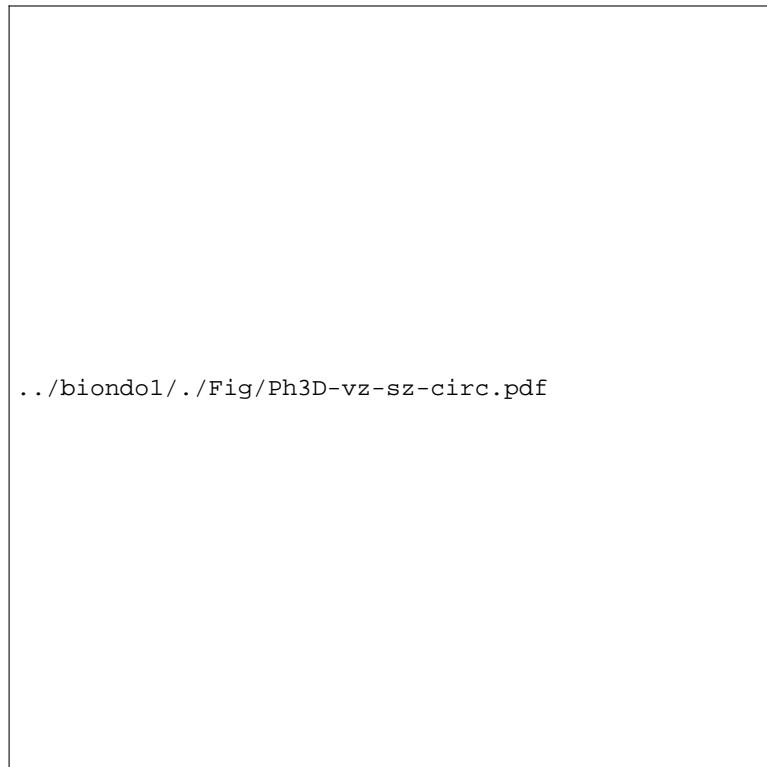


Figure 6: Depth slice of the migration results of the vertical gradient data set. A circle is overlaid onto the seismic data to visually verify the isotropy of the migrated dome.



Figure 7: In-line section of the migration results for the oblique gradient data set. This section passes through the middle of the dome.



Figure 8: Depth slice of the migration results of the oblique gradient data set. Frequency content and amplitude variations are evident along the circular reflector. However, the imaged reflector is fairly close to be circular.

common-azimuth downward continuation operator. The second one is a ray-theoretical interpretation of common-azimuth downward continuation that enables us to analyze the errors in presence of ray bending caused by velocity inhomogeneities.

We implemented common-azimuth depth migration by downward continuation in mixed space-wavenumber domain using a split-step scheme. The application of our depth migration algorithm to a data set with a strong horizontal component of the velocity gradient resulted in an accurate imaging of the reflectors.

ACKNOWLEDGEMENTS

We thank Arnaud Berlioux for helping to generate the dome model using GOCAD. Biondo Biondi would like to thank Norm Bleistein for a short conversation that motivated him to better understand the errors involved in the stationary-phase derivation of common-azimuth migration.

REFERENCES

- Audebert, F., 1994, 3-D pre-stack depth migration: Why Kirchhoff?: SEP-80, 191–208.
- Biondi, B., and Chemingui, N., 1994, Transformation of 3-D prestack data by Azimuth Moveout (AMO): 64th Annual Internat. Mtg., Soc. Expl. Geophys., Submitted.
- Biondi, B., and Palacharla, G., 1994a, 3-D prestack migration of common-azimuth data: SEP-80, 109–124.
- Biondi, B., and Palacharla, G., 1994b, 3-D prestack migration of common-azimuth data: 64th Ann. Internat. Meeting, Soc. Expl. Geophys., Expanded Abstracts, 1175–1178.
- Bleistein, N., 1984, *Mathematical methods for wave phenomena*: Academic Press.
- Claerbout, J. F., 1985, *Imaging the Earth's Interior*: Blackwell Scientific Publications.
- Gazdag, J., and Sguazzero, P., 1984, Migration of seismic data by phase-shift plus interpolation: *Geophysics*, **49**, no. 2, 124–131.
- Ikelle, L. T., 1991, Linearized inversion of 3-D multioffset marine seismic data: Proceedings, IEEE UK and RI Signal Processing Chapter, 1991 International Workshop on parallel architectures for seismic data processing, Glasgow, Scotland.
- Ratcliff, D. W., Jacewitz, C. A., and Gray, S. H., 1994, Subsalt imaging via target-oriented 3-D prestack depth migration: *The Leading Edge*, **13**, no. 3, 163–170.
- Stoffa, P. L., Fokkema, J., de Luna Freire, R. M., and Kessinger, W. P., 1990, Split-step fourier migration: *Geophysics*, **55**, no. 4, 410–421.

Western, P. G., and Ball, G., 1991, 3-D Pre-stack depth migration in the Gulf of Suez: a case history: 53rd Mtg. Eur. Assoc. Expl Geophys., Abstracts.

APPENDIX A

The purpose of this Appendix is to demonstrate the equivalence of the stationary phase derivation of the common-azimuth downward continuation operator [equation (7) in the main text] and the constraint on the propagation directions of the source rays (p_{sx}, p_{sy}, p_{sz}) and receiver rays (p_{rx}, p_{ry}, p_{rz}) expressed in equation (8).

We start by showing that equation (8) is directly derived by imposing the condition that the source ray and the receiver ray lie on the same plane. For this condition to be fulfilled, the components of the two rays in the direction of the cross-line axis y must be equal. From elementary geometry, these components are

$$\begin{aligned} dy_s &= v(\mathbf{s}, z) p_{sy} dl_s = \frac{p_{sy} dz}{p_{sz}} \\ dy_r &= v(\mathbf{r}, z) p_{ry} dl_r = \frac{p_{ry} dz}{p_{rz}}, \end{aligned} \quad (\text{B-1})$$

where dl_s, dl_r are the differential ray-paths lengths for the source and receiver rays, dy_s, dy_r are their components along the y axis, and dz is the component along the depth axis, constrained to be the same for the source and receiver rays. By equating the two equations in (B-1) we immediately derive equation (8); that is,

$$\frac{p_{sy}}{p_{sz}} = \frac{p_{ry}}{p_{rz}}. \quad (\text{B-2})$$

The second step is to eliminate p_{sz} and p_{rz} from equation (B-2) by using the following relationships among the ray parameters

$$\begin{aligned} p_{sx}^2 + p_{sy}^2 + p_{sz}^2 &= \frac{1}{v(\mathbf{s}, z)^2} \\ p_{rx}^2 + p_{ry}^2 + p_{rz}^2 &= \frac{1}{v(\mathbf{r}, z)^2} \end{aligned} \quad (\text{B-3})$$

After a few simplifications we get the equivalent of the stationary path relationship [equation (7)] but expressed in terms of ray parameters,

$$(p_{ry} - p_{sy}) = (p_{ry} + p_{sy}) \frac{\sqrt{\frac{1}{v(\mathbf{r}, z)^2} - p_{rx}^2} - \sqrt{\frac{1}{v(\mathbf{s}, z)^2} - p_{sx}^2}}{\sqrt{\frac{1}{v(\mathbf{r}, z)^2} - p_{rx}^2} + \sqrt{\frac{1}{v(\mathbf{s}, z)^2} - p_{sx}^2}}. \quad (\text{B-4})$$

To derive equation (7) from equation (B-4) it is sufficient to substitute for the ray parameters by applying the relationships

$$\begin{aligned} k_{mx} &= k_{rx} + k_{sx} = \omega(p_{rx} + p_{sx}) \\ k_{my} &= k_{ry} + k_{sy} = \omega(p_{ry} + p_{sy}) \\ k_{hx} &= k_{rx} - k_{sx} = \omega(p_{rx} - p_{sx}) \\ k_{hy} &= k_{ry} - k_{sy} = \omega(p_{ry} - p_{sy}) \end{aligned} \quad (\text{B-5})$$

